

ASSESSMENT OF InGaSb CRYSTALS BY CATHODO-LUMINESCENCE MICROSCOPY AND SPECTROSCOPY

M. F. Chioncel, C. Díaz-Guerra, J. Piqueras*, N. Duhanian^a, T. Duffar^a

Departamento de Física de Materiales, Facultad de Ciencias Físicas, Universidad Complutense de Madrid, 28040 Madrid, Spain

^aEPM-MADYLAM/ENSHMG, BP 35, 38042 St Martín d'Hères, France

Low band-gap InGaSb crystals are of interest for the development of thermo-photo-voltaic (TPV) cells and other devices operating in the infrared spectral range. In this work, cathodoluminescence (CL) in the scanning electron microscope (SEM) has been applied to study the homogeneity of InGaSb material grown by the vertical Bridgman technique with regard to effective incorporation of In to the ternary alloy and the nature and distribution of defects influencing the luminescence properties of this semiconductor. Back-scattered electron imaging and wavelength dispersive X-ray mapping were used as complementary techniques to CL for analysis of chemical composition and element distribution. The results show that local CL spectra provide information on the effective formation of the alloy, not revealed by other techniques.

(Received January 28, 2004; accepted February 19, 2004)

Keywords: Cathodoluminescence, InGaSb, Defect formation, TPV cells

1. Introduction

GaSb based compounds, in particular InGaSb and InGaAsSb, are of interest as low band-gap materials with applications in photovoltaic cells [1,2] or other devices operating in the infrared range. In particular, GaSb-based Thermo-Photo-Voltaic (TPV) cells converting a large part of infrared radiation are susceptible to produce high efficiencies and high power output densities [3,4]. One of the purposes is to match the band gap of the photovoltaic device to the peak output of the heat source. Since the radiator emission is mainly in the long wavelength range, low band-gap photovoltaic cells are used. The band gap of the alloy determines the spectral response and photovoltage of the cell, and is thus one of the most important cell parameters from the point of view of system design [5]. In this case, the gap can be adjusted by controlling the In content. For this reason, efforts are being devoted to grow crystals of the semiconductor alloy GaSb-InSb as perfect as possible and with InSb content of at least 10% as basic material for the cell. However, the growth of high-quality InGaSb crystals is difficult due to chemical segregation and the associated internal mechanical stresses [6-8]. Strong efforts have been undertaken to grow compositionally uniform, crack-free materials under different gravity conditions [9,10] or in terrestrial condition under high magnetic fields [11]. An increasing concern and interest in device performance-limiting factors calls for a spatially-resolved characterisation technique capable to provide a direct insight into InGaSb material properties.

In this work, cathodoluminescence (CL) in the scanning electron microscope (SEM) has been used to investigate the homogeneity of InGaSb grown by the vertical Bridgman method, as referred to effective incorporation of In to the ternary alloy as well as to the nature and distribution of defects influencing the luminescence of the material. CL studies of InGaSb have to our knowledge still not been undertaken. Other SEM-based techniques, as back-scattered electron (BSE) imaging and

* Corresponding author: piqueras@fis.ucm.es

wavelength dispersive X-ray microanalysis (WDS) were used as complementary techniques to CL for the analysis of chemical composition and element distribution.

2. Experimental

2.1. Crystal growth

An In GaSb ingot has been grown by the vertical Bridgman technique. Pure (9N) Ga, In and Sb have been mixed and solidified under controlled convection [8]. The most homogeneous, first to freeze part of this sample, 10 cm long, has been cut, drilled and etched in order to fit into the 12 mm boron nitride crucible. Atomic adsorption analysis of slices taken from top and bottom sides of the sample have shown a mean composition of 9 mol % InSb / 91 % GaSb. This ingot has been directionally solidified in the ground-engineering model of the Advanced Gradient Heating Facility provided by the European Space Agency. The growth procedure was identical to the LMS-AGHF-ESA8 space experiment [12] with a growth rate of 1 $\mu\text{m/s}$ under a thermal gradient of 33 $^{\circ}\text{C/cm}$ [13].

2.2. Characterization techniques

The cylindrical ingot was longitudinally cut in two parts and chemo-mechanically polished. Chemical etching reveals that the solid liquid interface has been more and more concave (seen from the liquid) all along the solidification, probably because of the increasing In concentration towards the axis. The sample was characterised by secondary electron (SE), BSE, WDS and CL modes of the SEM. WDS mappings and quantitative microanalysis were performed in a Jeol JXA-8900M Superprobe. The same SEM was used for BSE imaging of the analysed areas. CL measurements were carried out in a Hitachi S-2500 SEM with a cooled ADC Ge detector able to detect the CL signal from $\text{In}_x\text{Ga}_{1-x}\text{Sb}$ with a maximum x value of 0.22. Measurements were performed at 90 K using a 25 kV accelerating voltage. Spectra were recorded from areas showing mixed bright-dark CL contrast, selected areas of enhanced or low CL signal and spots of known chemical composition. CL emission bands were determined from the best fits to experimental spectra, using a sum of Gaussian line distributions. The In content was calculated from the position of the luminescence peaks attributed to the band gap transition in the ternary alloy [14].

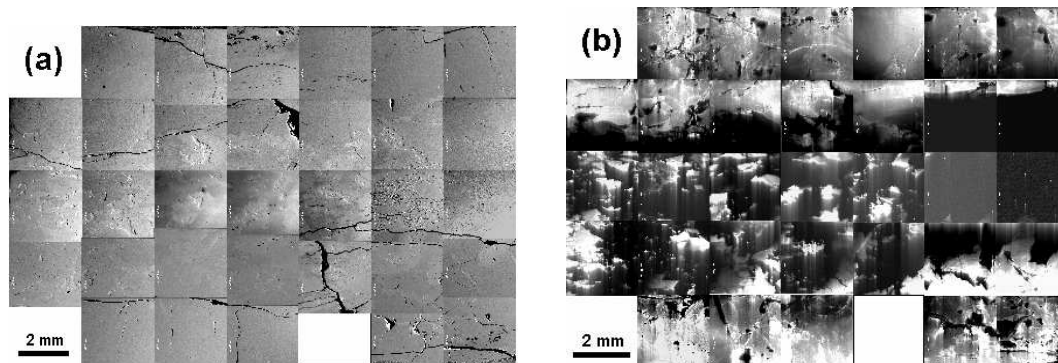


Fig. 1. SE (a) and CL (b) of the longitudinal section of the $\text{In}_x\text{Ga}_{1-x}\text{Sb}$ ingot. The images reveal a complex surface morphology and a non-homogeneous distribution of radiative recombination centres along both the radial and growth axis.

3. Results and discussion

The whole sample surface was mapped in the SE and CL modes while several representative areas were also imaged by BSE and WDS. The SE mapping of the sample [Fig. 1 (a)] show various types of surface morphology while panchromatic CL images reveal high inhomogeneity in the

distribution of the radiative recombination centres along both the radial and the growth axis, as shown in Fig. 1 (b). The SE micrographs show smooth, featureless surfaces in the proximity of the ingot lateral surface, corresponding to an enhanced CL emission. The inner part of the section shows a more complex morphology. This region consists of a distribution of luminescent areas. The top part of the sample is characterised by quenched CL emission while a fine texture is observed in the SE micrographs.

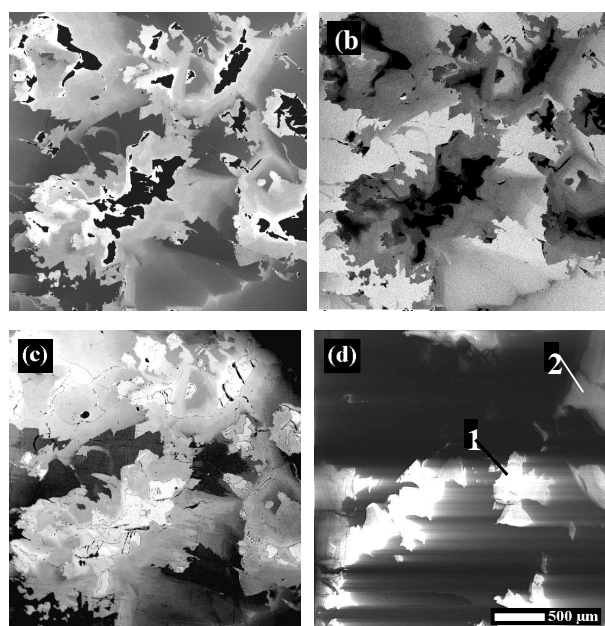


Fig. 2. Indium (a) and Gallium (b) WDS mappings of a central area marked in Fig. 1 and corresponding BSE (c) and CL (d) micrographs. Darker tones in X-ray mappings indicate a lower content of the element.

Several regions showing different topographic features were selected for BSE and WDS measurements. X-ray maps reveal the existence of areas of inhomogeneous chemical composition. BSE and SE micrographs images show a similar contrast, although such contrast appears enhanced in the former images. Fig. 2 shows the distribution of In (a), Ga (b) and the corresponding BSE (c) and CL (d) images of a selected area marked in Fig. 1. X-ray maps indicate the existence of some areas of pure Sb, bordered by narrow areas of pure In. An overall trend of In atoms agglomerating around areas of pure Sb was observed in all the regions investigated by WDS. The complex surface topography revealed by SE imaging and the lack of uniform distribution of the radiative recombination centres seem to be due to variation of the chemical composition. Radial segregation caused by curvature of the solid-liquid is known to induce high inhomogeneity along the ingot radius [8,15]. The enhanced CL emission in the proximity of the lateral surface of the cylinder is due to the existence of GaSb. CL spectra of this region are similar to those previously reported for pure GaSb [16]. In the central area, In started to incorporate during growth, leading to the formation of InSb and $\text{In}_x\text{Ga}_{1-x}\text{Sb}$ with varying x . Some cracks at the border of this region are probably due to segregation and subsequent supercooling of regions with higher In concentration [8]. The central zones showing an enhanced CL signal correspond to a mixture of GaSb and $\text{In}_x\text{Ga}_{1-x}\text{Sb}$ of low x ($x < 0.2$), while the surrounding area is a mixture of pure Sb, InSb and $\text{In}_x\text{Ga}_{1-x}\text{Sb}$, ($x > 0.2$). CL contrast observed in higher magnification images (Fig. 3) was not always related to morphological features or chemical heterogeneity. Some micrographs show the well-known “dot and halo” CL contrast associated to decoration of dislocation lines [17] while contrast related to boundaries was observed in other CL images.

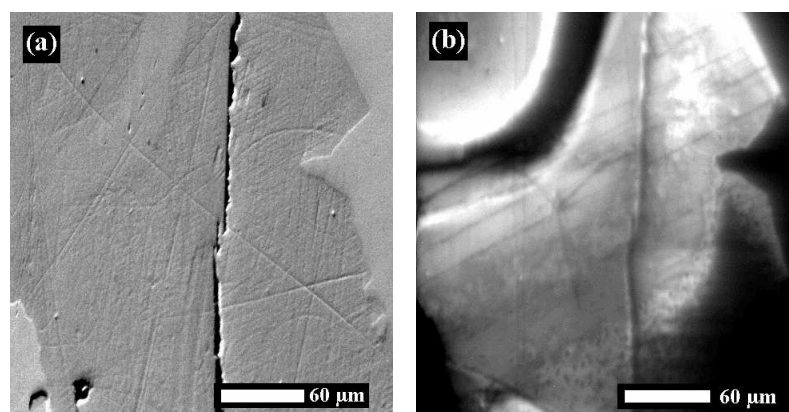


Fig. 3. SE image (a) and corresponding CL micrograph (b) of a central region of the InGaSb ingot. Dot and halo contrast related to emerging points of dislocation lines can be appreciated in the lower part of the CL image.

CL spectra recorded in distinct areas of very intense emission have identical appearance, showing a dominant peak centred at about 795 meV corresponding to the GaSb band edge transition (Fig. 4, position 1). Spots of lower CL emission and chemical composition determined by WDS were also selected for CL spectral analysis. These spectra reveal low energy shoulders which could be attributed, considering the WDS results, to $\text{In}_x\text{Ga}_{1-x}\text{Sb}$. An example is shown in Fig. 4, position 2, where such shoulder can be observed centred at about 740 meV. This peak would correspond to the ternary alloy with an In content $x \approx 0.06$. In addition, an overall red-shift of the CL maximum, that appears at about 780 meV, is observed. Gaussian deconvolution of the spectrum shown in Fig. 4 (curve 2) reveals that the main broad CL emission is actually due to overlapping of two bands centred near 770 meV and 790 meV, which could be respectively attributed to $\text{In}_x\text{Ga}_{1-x}\text{Sb}$ of low In content ($x \approx 0.02$) and the GaSb band gap transition. Some of these spectra also show a weaker emission near 820 meV, previously related in GaSb to tail states and shallow acceptors [18]. It was found that the position and the relative intensities of the observed emission peaks changed slightly from spot to spot. The previous results indicate that the excitation volume, beneath the targeted spot, contains GaSb and $\text{In}_x\text{Ga}_{1-x}\text{Sb}$ of different x . Although such spectra reveal the presence of the ternary alloy, there is generally a disagreement between the In contents calculated from the positions of our CL emission bands and those determined by X-ray quantitative measurements. Actually, WDS measurements indicate a higher In content, as compared with that revealed by CL spectroscopy. Since the X-ray measurements reveal the total In content while the CL spectra provide the In content in the ternary compound, this shows a reduced incorporation of In to form the ternary alloy. Such correlative measurements, carried out in the same spots of the sample, emphasise the unique capabilities of the CL technique for analysing with high spatial resolution the quality of $\text{In}_x\text{Ga}_{1-x}\text{Sb}$ crystals and the efficiency of In incorporation in the lattice.

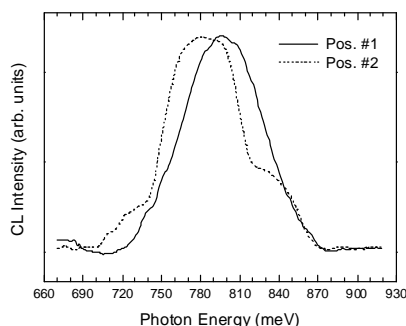


Fig. 4. Spectra from spots of enhanced (position 1) and low (position 2) CL signal marked in Fig. 2 (d).

4. Conclusions

CL in the SEM has been used for homogeneity assessment of InGaSb material grown by the vertical Bridgman method. CL micrographs and X-ray mappings reveal chemical inhomogeneity both along and across the longitudinal ingot section. In particular, the different degree of In incorporation along and across the ingot is revealed by the CL spatial and spectral measurements. Areas of enhanced CL signal, formed by GaSb and $\text{In}_x\text{Ga}_{1-x}\text{Sb}$ with $x < 0.2$, were observed in the central part of the sample. Measurements of the band gap energy from the CL spectra allowed us to determine the In content of the semiconductor ternary alloy. The obtained results differ from those obtained by X-ray microanalysis, showing the capability of CL spectroscopy to monitor the effective incorporation of In to the matrix with high spatial resolution.

Acknowledgements

This work was carried out in the frame of the Fifth Framework European Programme for research; HPRN-CT 2001-00199 project. MFC acknowledges European Commission for financial support.

References

- [1] J. P. Benner, T. J. Coutts, D. S. Ginly (eds.) Proc. 2nd NREL Conf. on Thermophotovoltaic Generation of Electricity, AIP Conf. Proc. **358**, (1995).
- [2] T. J. Coutts, C. S. Allma, J. B. Benner (eds.) Proc. 3rd NREL Conf. on Thermophotovoltaic Generation of Electricity, AIP Conf. Proc. **401**, (1997).
- [3] O. V. Sulima, A. W. Bett, P. S. Dutta, M. G. Mauk, R. L. Mueller, 29th Photovoltaic Specialists Conference, May 20-24, New Orleans (2002).
- [4] N. P. Uppal, G. Carache, P. Baldasaro, B. Campbell, S. Loughin, S. Svensson, D. Gill, J. Cryst. Growth **175-176**, 877 (1997).
- [5] M. G. Mauk, V. M. Andreev, Semicond. Sci. Technol. **18**, S191 (2003).
- [6] D. Auvergne, J. Camassel, H. Mathieu, A. Joullie, J. Phys. Chem. Sol. **35**, 133 (1974).
- [7] S. Sen, R. A. Lefer, W. R. Wilcox, J. Cryst. Growth **43**, 526 (1978).
- [8] C. Marín, P. S. Dutta, E. Diéguez, P. Dussere, T. Duffar, J. Cryst. Growth **173**, 271 (1997).
- [9] J. F. Yee, M. C. Lin, K. Sarma, W. R. Wilcox, J. Cryst. Growth **30**, 185 (1975).
- [10] T. Duffar, M. D. Serrano, C. D. Moore, J. Camassel, S. Contreras, P. Dussere, A. Rivallant, B. K. Tanner, J. Cryst. Growth **192**, 63 (1998).
- [11] Y. Hayakawa et al. J. Cryst. Growth **213**, 40 (2000).
- [12] N. Duhanian, C. Marín, T. Duffar, J. Abadie, M. Chaudet, E. Diéguez, Microgravity Science and Technology **XI/4**, 187 (1997).
- [13] N. Duhanian, Ph. D. Thesis, Université Paris (1998).
- [14] C. H. Su, Y. K. Su, F. S. Juang, Solid State Electronics **35**, 1385 (1992).
- [15] P. S. Dutta, A. Ostrogorsky, J. Cryst. Growth **217**, 360 (2000).
- [16] P. Hidalgo, B. Méndez, P. S. Dutta, J. Piqueras, E. Diéguez, Phys. Rev. B **57**, 6479 (1998).
- [17] B. G. Yacobi, D. B. Holt, Cathodoluminescence Microscopy of Inorganic Solids, Plenum Press, New York, (1990).
- [18] G. Benz, R. Conradt, Phys. Rev. B **16**, 843 (1977).